Mineralogy and geochemistry of silicate dyke rocks associated with carbonatites from the Khibina complex (Kola, Russia) – isotope constraints on genesis and small-scale mantle sources*

S. Sindern[1,7], **A. N. Zaitsev**[2,8], **A. Demény**[3], **K. Bell**[4],
A. R. Chakmouradian[5], **U. Kramm**[1], **J. Moutte**[6], and **A. S. Rukhlov**[4]

[1] Institut für Mineralogie und Lagerstättenlehre – RWTH, Universität
Aachen, Germany
[2] Department of Mineralogy, St. Petersburg State University, Russia
[3] Laboratory for Geochemical Research, Hungarian Academy of Sciences,
Budapest, Hungary
[4] Ottawa-Carleton Centre for Geoscience Studies, Department of Geology,
Carleton University, Ottawa, Ontario, Canada
[5] Department of Geological Sciences, University of Manitoba, Winnipeg, Canada
[6] Ecole des Mines, Centre SPiN, Saint Etienne, France
[7] Institut für Mineralogie, WWU-Münster, Germany
[8] Institut für Mineralogie, Petrologie und Geochemie, Universität Freiburg,
Germany

Summary

The eastern part of the agpaitic Khibina complex is characterized by the occurrence of dykes of various alkali silicate rocks and carbonatites. Of these, picrite, monchiquite, nephelinite and phonolite have been studied here. Whole rock and mineral geochemical data indicate that monchiquites evolved from a picritic primary magma by olivine + magnetite fractionation and subsequent steps involving magma mixing at crustal levels. None of these processes or assimilation/magma mixing of wall rocks or other plutonic rocks within the complex can entirely explain the geochemical and Nd–Sr-isotopic

---

* Supplementary material to this paper is available in electronic form at http://dx.doi.org/10.1007/s00710-003-0016-2

characteristics of the monchiquites (i.e. a covariant alignment between $(^{87}Sr/^{86}Sr)_{370} = 0.70367$, $(^{143}Nd/^{144}Nd)_{370} = 0.51237$ and $(^{87}Sr/^{86}Sr)_{370} = 0.70400$, $(^{143}Nd/^{144}Nd)_{370} = 0.51225$ representing the end points of the array). This signature points to isotopic heterogeneities of the mantle source of the dyke-producing magma. The four mantle components (i.e. depleted mantle, lower mantle plume component, EMI-like component and EMII-like component) must occur in different proportions on a small scale in order to explain the isotopic variations of the dyke rocks. The EMII-like component might be incorporated into the source area of the primary magma by carbonatitic fluids involving subducted crustal material. The most likely model to explain the small-scale isotopic heterogeneity is plume activity. The results of this study do not provide any support to a cogenetic origin (e.g. fractionation or liquid immiscibility) for carbonatite and monchiquite or other alkali-silicate dyke rocks occurring in spatial proximity. Instead, we propose that both, carbonatite and picrite/monchiquite, originated by low-degree partial melting of peridotite. Textural observations, mineralogical data, and C and O isotopic compositions suggest incorporation of calcite from carbonatite in monchiquite and the occurrence of late-stage carbothermal fluids.

Introduction

The spatial and temporal association of silicate rocks such as lamprophyres, melanephelinites, melilitites, nephelinites and phonolites on one side and carbonatites on the other side has been documented from many localities, e.g. Fen (*Dahlgren*, 1994), Igaliko (*Pearce* and *Leng*, 1996), Kandalaksha (*Beard* et al., 1996; *Ivanikov* et al., 1998), Dalbykha (*Kogarko*, 1997), Buhera (*Harmer* et al., 1998). Published mineralogical and geochemical data suggest that the relationship between carbonatites and silicate rocks is complex. The rocks may be genetically related, and the two-magma types (silicate and carbonate) produced by liquid immiscibility/or magma differentiation. Alternatively, they may originate from different mantle sources, with carbonatites being derived directly by evolution of mantle-derived primary carbonate magma (e.g. *Bell*, 1998; *Harmer* and *Gittins*, 1998). In many cases associated silicate rocks show open-system behaviour including magma mixing and contamination from a continental crust (e.g. *Simonetti* and *Bell*, 1994; *Dunworth* and *Bell*, 2001).

One example of a carbonatite–silicate rock association is the Khibina alkaline complex in the Kola Peninsula, Russia (Fig. 1). At Khibina, the plutonic silicate rocks include peridotites, clinopyroxenites, layered ijolites, urtites and melteigites and associated apatite–nepheline rocks, and various nepheline syenites. Numerous nepheline–syenitic pegmatites and dykes of lamprophyres, melanephelinites, nephelinites and phonolites crosscut the plutonic series (e.g. *Kostyleva-Labuntsova* et al., 1978; *Arzamastsev* et al., 1988; *Khomyakov*, 1995).

Carbonatites, found in drill cores at the eastern part of the complex, form a stockwork that shows a great variety of both silicate–carbonate and predominantly carbonate rocks. The geological setting and mineralogy of the Khibina carbonatites are well established (*Dudkin* et al., 1984; *Zaitsev*, 1996; *Zaitsev* et al., 1998). The carbonatites have significantly different Sr–Nd isotopic compositions in comparison with the nepheline syenites and foidolites, suggesting that they were derived from different parent magmas (*Kramm* and *Kogarko*, 1994; *Zaitsev* et al., 2002). However, little is known about the genetic relationship between the carbonatites
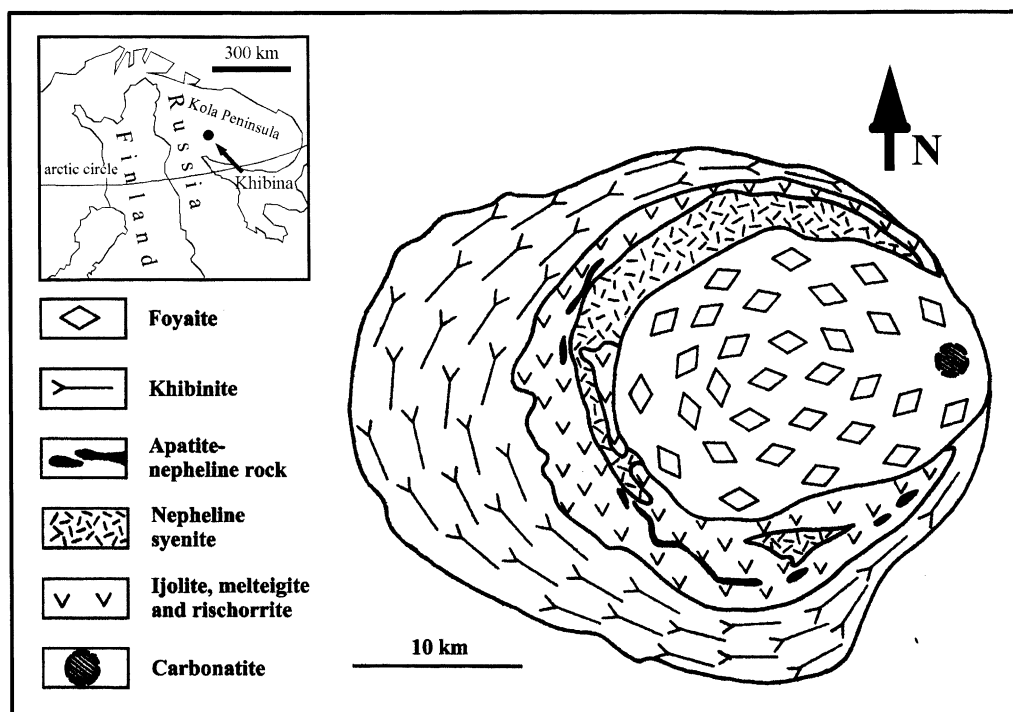
Fig. 1. Simplified geological map of the Khibina complex. Circle shows the area where carbonatite and alkali silicate dykes occur. Inset shows position of the Khibina complex on the Kola Peninsula

and alkali silicate dyke rocks, and the key to understanding the genesis of the Khibina carbonatites might be found in the close spatial association between the carbonatites and dyke rocks, which are both abundant in the eastern part of the Khibina pluton.

Here, we present the results of geochemical, mineralogical and isotopic studies of these silicate dyke rocks in an attempt to unravel the nature of the source that generated the parent magmas to these rocks and to constrain the relationship between the silicate dyke rocks and associated carbonatites.

Geological setting

Only drill-core material is available from the eastern part of the Khibina complex. Geological reconstruction of this material is extremely difficult due to strong syn-magmatic tectonism in this area, which produced wide-spread brecciation and faulting.

Leucocratic nepheline syenite is the dominant silicate rock in this area. It is medium-grained massive rock with modal and whole-rock chemical compositions similar to those of other nepheline syenites found elsewhere in the Khibina complex (*Kostyleva-Labuntsova* et al., 1978). Ijolite and clinopyroxenite occur as xenoliths (5 cm–20 m) in the foyaites (see Fig. 1 in *Zaitsev*, 1996). In terms of the whole-rock chemistry, the ijolite in xenoliths is similar to the ijolite from the central part of the massif, i.e. the so-called ijolite–urtite arc (*Kostyleva-Labuntsova* et al., 1978).

All of the above plutonic series within the complex are cut by dykes of various silicate rocks ranging from 10 cm to 10 m in thickness. We recognize four groups of dykes from this area. These are represented by (from oldest to youngest): alkali picrite, monchiquite, nephelinite and phonolite. Monchiquite is also observed as small (0.5–1 cm across) xenoliths in phonolite, surrounded by a reaction rim of mica. Picrite and nephelinite are rare, whereas monchiquite and phonolite are common. In addition to dykes, the presence of a stock-like body of phonolite, 150–200 m in diameter, has been suggested on the basis of geophysical data and supported by data from drilling (*Dudkin* et al., 1984).

In the eastern part of the Khibina complex, the carbonatitic rocks are among the youngest to crystallize. They form veins from 0.5 cm to 4 m in thickness and cross-cut all plutonic and dyke silicate rocks. The temporal sequence of the carbonatitic rocks is as follows: (1) phoscorite-like rocks, (2) calcite carbonatites, (3) REE-rich calcite, calcite–ankerite, kutnohorite and rhodochrosite–siderite carbonatites, and (4) REE-rich carbonate–zeolite rocks (*Zaitsev*, 1996). The rocks were interpreted to be polygenetic in origin, showing a transition from a magmatic to a volatile-rich fluid carbohydrothermal system (*Zaitsev*, 1996). The carbonatites evolved chemically from calciocarbonatites (normal early sövitic and late REE-alkali-rich burbankite-bearing calcite carbonatites) through ferrocarbonatites (REE-rich calcite–ankerite and ankerite) to manganocarbonatites (REE-rich kutnahorite-bearing and rhodochrosite–siderite carbonatites) (*Zaitsev* et al., 1998).

Petrography of dyke rocks

Dykes are massive, porphyritic rocks mainly containing phenocrysts of olivine, clinopyroxene and mica in the picrite and monchiquite, of clinopyroxene, mica and nepheline in the nephelinite, and of feldspar, clinopyroxene, nepheline (or cancrinite) in the phonolite. The monchiquite also contains discrete subhedral crystals of calcite and globular patches up to 1 mm in diameter, composed of subhedral calcite in the core that is commonly surrounded by mica and pyroxene ± magnetite. The phenocrysts are set in a fine-grained groundmass that consists of clinopyroxene, mica, apatite and opaque minerals (chromite, magnetite and perovskite) in the picrite and monchiquite, and nepheline and titanite in the nephelinite and phonolite. Ilmenite is a common accessory late-stage mineral in all varieties of the dyke rocks. Secondary minerals, e.g. magnesite and serpentine after olivine, cancrinite after nepheline, are also abundant. Fine calcite veinlets crosscut some of the dyke rocks. Noteworthy is the occurrence of various rare minerals enriched in REE, Ba and Sr, such as ancylite-(Ce), barytocalcite, carbocernaite, burbankite, synchysite-(Ce) and monazite-(Ce). With the exception of burbankite, occurring as blebs in apatite, these minerals form poikilitic anhedral crystals (10–120 μm) that replaced silicate minerals.

Mineralogy

For clinopyroxene and calcite chemical data, microprobe analytical procedures and color CL photos are given as electronic supplementary material (referred to as e.g. Table 1S or Fig. 1S). Mineralogical descriptions and chemical data for olivine, mica, andradite, nepheline, cancrinite and alkali-feldspar, spinel-group minerals,
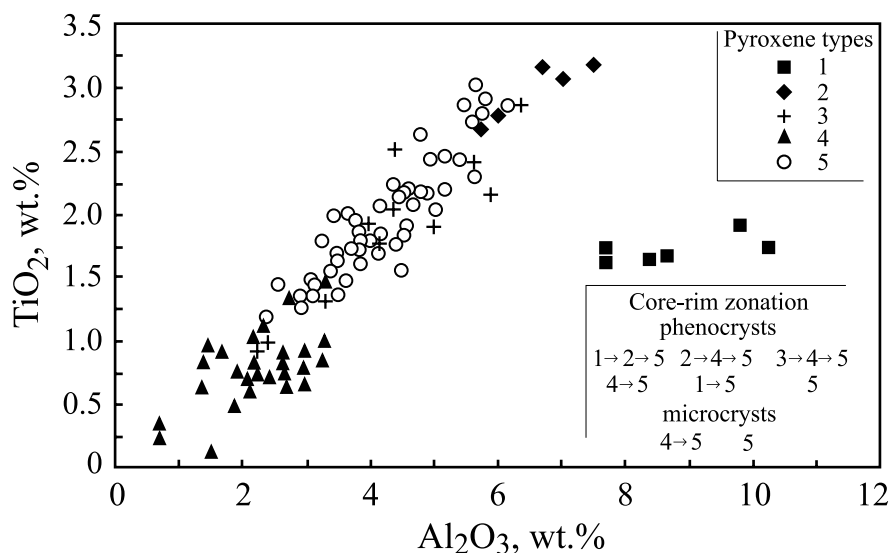
Fig. 2. Plot of Al_2O_3 vs. TiO_2 (wt.-%) in clinopyroxene from monchiquites. The inset shows clinopyroxene types occurring in zoning successions. See text for explanation of pyroxene types

ancylite-(Ce) and synchysite-(Ce), perovskite and ilmenite are completely presented as electronic supplementary material, too.

Clinopyroxene

Phenocrysts and microphenocrysts of this mineral are typically zoned; normal, reverse and oscillatory zoning can commonly be seen along the core-rim boundary. Cores of some crystals show resorption and are commonly not in optical continuity with the rim. Microscopic observations and the mineral chemistry suggest the presence in the monchiquite of 5 varieties of clinopyroxene differing in colour and TiO_2, Al_2O_3, Cr_2O_3 and Na_2O contents (Table 2S, Fig. 2). These varieties are:

(1) subsilic aluminian diopside (colourless core in the phenocrysts); (2) subsilic aluminian diopside (colourless core and inner rim in the phenocrysts, higher Ti-content than type 1); (3) aluminian chromian diopside (colourless to light green core and inner rim in the phenocrysts); (4) aluminian aegirine–augite (green to dark green core and inner rim in pheno- and microphenocrysts); (5) aluminian diopside (colourless core, inner and outer rim in pheno- and microphenocrysts).

Diopside of types 1 and 2 is rare and observed only in the Mg-rich monchiquites. Chromian diopside (type 3) was found only in two crystals from two monchiquite samples, whereas diopside of type 5 and aegirine–augite of type 4 are ubiquitous in all monchiquite samples. Many type-4 clinopyroxenes have rims with a low Na_2O content and can thus be termed ''green-core clinopyroxenes''.

The various clinopyroxene types are characterized by different Mg#'s. Types 2, 3 and 5 have Mg#'s ranging between 0.89 and 0.93, whereas types 1 and 4 have relatively low Mg#'s of 0.74 and 0.71, respectively. Figure 2 shows a positive correlation between Al_2O_3 and TiO_2 in most of the crystals, with types 2 and 4

representing the Al–Ti-rich and Al–Ti-poor end-members, respectively. An exception is the type-1 diopside, which lies in the Al-enriched and Ti-depleted part of the diagram.

The calculated distribution of Al between octahedral and tetrahedral sites shows that the clinopyroxenes from the monchiquites (Table 2S) are characterized by different $^{VI}Al/^{IV}Al$ ratios. The type-1 diopside and type-4 aegirine–augite have high $^{VI}Al/^{IV}Al$ ratios of 0.42–0.56 and 0.18–0.56, respectively (with one analysis showing 1.13). Other types (diopside 2, 3 and 5) have $^{VI}Al/^{IV}Al$ ratios lower than 0.09. For diopsidic pyroxenes these can be interpreted in terms of crystallisation pressures. $^{VI}Al/^{IV}Al$ ratios lower than 1.0 point to formation under pressures lower than 10 kbar (*Aoki* and *Shiba*, 1973; *Wass*, 1979; *Bultitude* and *Green*, 1971; *Simonetti* et al., 1996). Types 2, 3 and 5 probably formed under lower pressures than types 1 and 4 and have high Mg#'s. They thus appear to be in or closer to an equilibrium with their monchiquitic host magma (*Grove* and *Barker*, 1984; *Morbidelli* et al., 2000). It has to be noted that the chromian diopside (type 3), which differs from lherzolithic clinopyroxenes by its lower Na_2O and Al_2O_3 contents, also seems to have equilibrated with the monchiquitic magma. However, the clinopyroxenes of types 1 and 4, found in the same rocks, have lower Mg#'s indicating formation in less primitive magmas under higher pressures and thus represent growth stages in a magma not represented by the monchiquite.

In line with the descriptions by *Duba* and *Schmincke* (1985) or *Dobosi* and *Fodor* (1992), the existence of the ''green-core'' type 4 pyroxene in the monchiquites points to polybaric evolution combined with episodes of magma mixing.

Calcite

Occurs as (i) euhedral phenocrysts, (ii) polycrystalline aggregates that compose cores of globules (amygdales) and (iii) microcrystalline spots in groundmass and fine veinlets. Not all monchiquite samples contain phenocrysts or globular calcite, but they all contain microcrystalline calcite (spots and veinlets) in the groundmass.

Euhedral phenocrysts of calcite are 300–700 µm in size. They are observed in monchiquite (sample 596/418.2) that does not contain calcite globules. The calcite grains show no disequilibrium relations with coexisting silicate minerals (Fig. 1AS–BS).

Calcite in globules occurs as small 50–250 µm subhedral crystals and monomineralic aggregates up to 1 mm in size (samples 625/118.9, 695/124.5, 625/218.8, Fig. 1CS–DS) which are similar to calcite crystals in a carbonatite xenolith occurring in the Oleni ultramafic lamprophyre (*Beard* et al., 1996). Typically calcite in globules is surrounded by mica, pyroxene and magnetite. Calcite in the globules shows typical yellow or orange–yellow CL-colours. In some cases, calcite aggregates are rimmed by 10–60 µm thick bands of calcite with a distinct dark-red CL-colour (Fig. 1DS). Disequilibrium relations observed between the minerals in the globules and the bands indicate a late-stage subsolidus origin of the calcite rim.

Microcrystalline spots of 5–10 µm in size are common in the groundmass of all studied samples (Fig. 1CS–DS). They are of deep red CL-colour and show heterogeneous distribution within the samples studied. Apart from the microcrystalline spots, veinlets ranging from 5 µm to 2 mm in thickness are common. The observed

textures suggest that this calcite variety also formed during late-stage subsolidus processes.

Euhedral calcite phenocrysts contain low levels of MnO, MgO, FeO, BaO and REE_2O_3 (all <0.2 wt.%). The SrO content is significant, ranging from 1.8 to 3.0 wt.% (Table 6S, analyses 1–3).

The calcite from globular segregations also shows low contents of MgO and FeO (<0.1 wt.%), and BaO (<0.2 wt.%). This variety is relatively enriched in MnO (0.4 to 0.5 wt.%) and REE_2O_3 (up to 0.4 wt.%). Compared to the phenocrystic calcite, the SrO content is lower, ranging from 0.7 to 0.8 wt.% (Table 6S, analyses 4–6). The calcite forming corrosion rims on the calcite segregations contains yet lower SrO (0.3–0.5 wt.%), but higher MgO (0.5–0.6 wt.%), FeO (0.4–0.7 wt.%) and MnO (1.2–1.3 wt.%) contents (Table 6S, analysis 7).

The calcite veinlets cutting dykes and microcrystalline calcite in the groundmass contain very low levels of SrO (<0.2 wt.%), whereas the MnO and FeO contents reach 0.5 and 0.8 wt.%, respectively (Table 6S, analysis 8).

The observed trace element distribution in calcite from the monchiquites is similar to those in carbonatitic rocks and carbonate-bearing silicate rocks where Sr-enrichment is in general characteristic of primary calcite, and secondary or late-stage calcite always shows depletion in Sr that can be accompanied by enrichment in $Mn \pm Fe$ (*Sokolov*, 1985; *Zaitsev*, 1996; *Zaitsev* and *Chakhmouradian*, 2002).

Geochemistry of dyke rocks

Whole-rock analyses for major, trace and RE elements are reported in Table 1. The analytical procedures are given as electronic supplement. The picrite and monchiquites are ultrabasic silica-poor rocks with 35.0–41.5 wt.% of SiO_2. The SiO_2 content increases to 46.1 wt.% in the nephelinite with a maximum of 52.9 wt.% in the phonolite. All silicate rocks are characterized by high contents of alkalis (7.3–8.7 wt.% $Na_2O + K_2O$ in the picrite and monchiquite, 12.5 wt.% in the nephelinite, and 13.1–16.4 wt.% in the phonolite). The rocks are characterised by variable Na_2O/K_2O ratios (0.63–2.39); the phonolite samples are sodic, picrite and nephelinite ultra-potassic, and monchiquites are potassic except for sample 699/255.6. CO_2 contents range from 0.64 to 11.80 wt.%.

Major element variations vs. MgO contents define two distinct groups: high-Mg (picrite, Mg# = 0.78; monchiquite, Mg# = 0.55–0.73), and low-Mg (nephelinite, Mg# = 0.37; phonolites, Mg# = 0.19–0.25). A broad negative correlation of MgO is observed with SiO_2, Al_2O_3, CaO, Na_2O and K_2O, and a positive with TiO_2 and FeO_{total} (Fig. 3).

The trace elements Ni and Cr show a strongly positive correlation with fractionation indicators such as the Mg#. Co and Sc are markedly higher in the monchiquites compared to the nephelinite and phonolites, whereas Nb shows an opposite distribution, >175 ppm in the nephelinite and phonolites, and <175 ppm in the monchiquite. Y, Ce, Ba, Sr, Rb, Th and Zr have overlapping concentrations with respect to the different lithologies.

Mantle-normalized element signatures for the picrite and monchiquites (Fig. 2AS) show enrichment in incompatible elements with slight positive or negative K anomalies and significant negative Zr and Ti anomalies. The patterns are similar to

Table 1. *Chemical composition of the alkaline ultrabasic silicate dykes.* * – all Fe as FeO

Sample rock	604/400 Picrite	Monchiquite					696/798 Nephelinite	Phonolite	
		625/218.8	695/124.5	625/118.9	596/418.2	699/255.6		633B/367	630/186.3
SiO_2	35.01	41.51	38.90	36.49	34.79	37.09	46.11	50.79	52.92
TiO_2	1.59	2.17	1.97	2.06	3.39	2.92	1.16	0.65	0.48
Al_2O_3	7.99	12.05	10.82	9.88	9.41	10.72	17.40	19.89	20.48
FeO^*	8.34	8.18	8.35	9.13	9.90	10.80	6.45	4.77	3.43
MnO	0.27	0.19	0.24	0.43	0.39	0.25	0.32	0.33	0.15
MgO	16.75	12.83	11.33	12.05	12.40	7.52	2.15	0.89	0.45
CaO	9.12	10.12	11.57	10.99	16.70	14.09	6.42	3.92	1.26
Na_2O	3.22	4.76	3.97	3.84	4.42	6.04	4.88	9.26	10.57
K_2O	5.12	3.08	3.66	5.65	2.88	2.66	7.61	3.88	5.85
P_2O_5	0.55	0.80	0.91	0.76	1.32	1.18	0.41	0.97	0.08
LOI	11.36	3.56	7.40	8.73	5.05	5.89	6.26	4.25	3.84
Total	99.33	99.24	99.13	100.00	100.65	99.16	99.16	99.60	99.52
CO_2	11.80	2.20	5.86	7.32	4.20	4.65	4.03	2.15	0.64
Mg#	0.78	0.73	0.70	0.70	0.69	0.55	0.37	0.25	0.19
Cr	1317	757	536	604	616	481	153	97	124
Ni	481	319	258	244	198	78	47	14	17
Co	51	51	49	45	55	56	27	9	11
Sc	23	18	18	23	26	23	3.9	2.1	0.5
V	307	186	209	266	258	319	178	67	52
Pb	8	10	26	15	18	10	38	20	34
Zn	36	31	38	29	33	38	58	19	35
Rb	183	108	118	115	85	94	261	125	118
Ba	1174	1795	1593	1967	1407	1617	3179	1378	925
Th	11	20	55	67	18	18	18	19	35
Sr	1315	1445	2397	1762	2869	2654	1165	1276	916
Nb	98	133	138	148	112	137	313	254	183
Zr	130	273	322	264	223	266	516	587	558
U	2	4	2	2	3	4	8	7	9
Ga	5	6	7	7	9	7	14	10	12
La	68.3	125	188	108	481	152	145	85	76
Ce	142	238	330	238	904	295	259	139	134
Nd	76.5	112	146	225	321	147	93.3	49	40.2
Sm	16.5	18.2	20.5	79.8	49.7	24.4	13.1	7.0	5.5
Eu	3.99	4.30	4.86	22.6	9.39	5.25	2.73	1.26	1.31
Gd	12.2	11.7	13.1	68.6	27.7	14.8	7.52	3.20	4.12
Dy	7.55	6.46	10.7	41.7	14.8	7.4	3.98	2.46	2.88
Er	3.12	2.41	8.1	18.4	6.3	2.79	1.59	1.19	1.13
Yb	2.23	2.41	7.09	11.9	4.65	1.72	1.49	1.09	1.59
Y	32.5	26	78.7	166	53.6	26.7	17.8	15.9	14.7

those shown by monchiquites from other localities (*Rock*, 1991). Mantle-normal-ized element signatures for the nephelinite and phonolites (Fig. 2BS) indicate enrichment in Nb, and Zr and depletion in P relative to the monchiquites. REE,
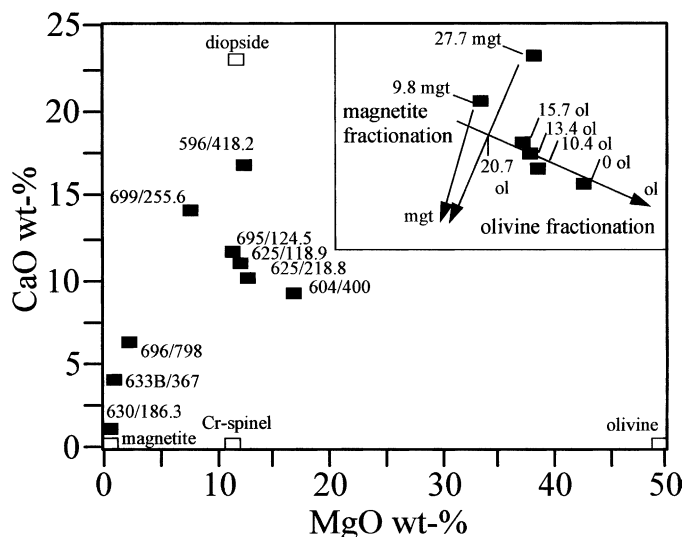
Fig. 3. Plot of CaO vs. MgO (wt.-%) of the dyke samples. Also shown are compositions of potential fractionating phases, indicating trends of olivine and magnetite fractionation. The inset shows calculated wt-percentages of fractionating olivine (ol) and magnetite (mgt) starting with a picrite defined by sample 604/400. The CaO- and MgO-contents of the monchiquites can be explained by olivine fractionation from a picrite magma. The composition of samples 699/255.6 and 596/418.2 can be explained by additional magnetite fractionation

Th and Ba are the trace elements that show significant variation in abundance from sample to sample.

Contents of RE elements show large variations between the samples, but are generally higher in the picrite, monchiquite and nephelinite (364.9–1872.1 ppm) compared with the phonolite (281.4–305.1 ppm). Chondrite-normalized REE signatures (Fig. 3S) show similar parallel patterns displaying a pronounced LREE enrichment with $(La/Sm)_{CN} = 2.4$–7.9 and $(La/Yb)_{CN} = 17.2$–66.9. An exception is the monchiquite 625/118.9 which shows enrichment in MREE with a $(La/Sm)_{CN}$ ratio of 0.8 and has the lowest $(La/Yb)_{CN}$ ratio of 5.9.

C–O isotope composition

Carbonates from monchiquites and nephelinite have been analysed for C–O-isotope composition. For analytical procedures, see electronic supplement. The results are given in Table 2 and plotted in Fig. 4.

Calcite from four monchiquite samples shows relatively small scale variations of $\delta^{13}C$ ranging between -5.5 and $-4.4‰$ relative to V-PDB, and $\delta^{18}O$ between 10.5 and 12.6‰ relative to V-SMOW. Only calcite from monchiquite 625/218.8 has a higher $\delta^{18}O$-value of 18.4‰. Calcite from the nephelinite has a slightly higher $\delta^{13}C$ value ($-4.0‰$) compared to the monchiquites, but its $\delta^{18}O$ value (12.6‰) falls within the range defined by calcite from the monchiquite. For comparison we also plotted in Fig. 4 data available for the carbonatites (both pristine and altered) and hydrothermal veins of the Khibina complex (*Khomyakov*, 1995; *Zaitsev*, 1996; *Pokrovskii* and *Kravchenko*, 2001; *Zaitsev* et al., 2002).

224 S. Sindern et al.

Table 2. Rb–Sr-, Sm–Nd-, $\delta^{18}O_{(VSMOW)}$- and $\delta^{13}O_{(VPDB)}$ – isotope data for monchiquite, nephelinite and phonolite samples

Rock	Sample	$^{87}Rb/^{86}Sr$	$^{87}Sr/^{86}Sr$ measured	$^{87}Sr/^{86}Sr$ initial	$\varepsilon_{Sr}(370)$	$^{147}Sm/^{144}Nd$	$^{143}Nd/^{144}Nd$ measured	$^{143}Nd/^{144}Nd$ initial	$\varepsilon_{Nd}(370)$	$\delta^{18}O‰$[1] (VSMOW)	$\delta^{13}C‰$[1] (VPDB)
Monchiquite	625/218.8	0.1888(4)	0.70489(2)	0.70390	−2.4	0.0889(2)	0.512535(15)	0.512320	3.1	18.4	−5.5
Monchiquite	695/124.5	0.1276(4)	0.70467(2)	0.70400	−1.0	0.0820(1)	0.512451(15)	0.512253	1.8	11.6	−4.4
Monchiquite	596/418.2	0.0747(4)	0.70414(2)	0.70375	−4.5	0.0751(1)	0.512551(15)	0.512369	4.1	11.5	−5.5
Monchiquite	699/255.6	0.0948(2)	0.70417(2)	0.70367	−5.6	0.0897(1)	0.512590(15)	0.512373	4.1	10.5	−4.4
Nephelinite	696/798	0.5500(50)	0.70661(3)	0.70371	−5.0	0.0758(2)	0.512496(15)	0.512312	2.9	12.6	−4.0
Phonolite	630/186.3	0.24422(7)	0.70537(3)	0.70408	0.3	0.0776(4)	0.512471(15)	0.512282	2.4		

[1] Stable isotope data obtained from calcite in monchiquite and nephelinite

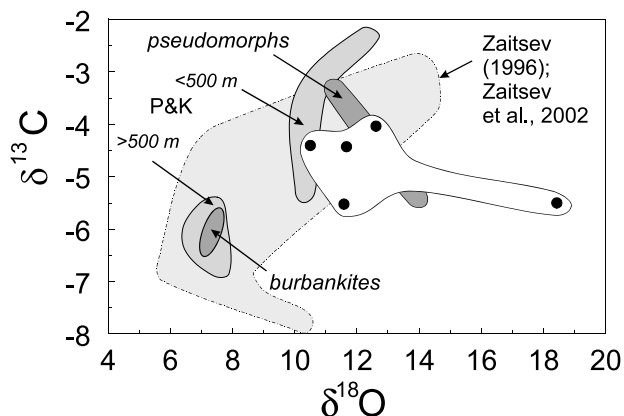Fig. 4. Plot of $\delta^{13}C$ (VPDB) vs. $\delta^{18}O$ (VSMOW) diagram showing values of calcite from monchiquite and nephelinite samples (dots) compared to signatures of Khibina carbonatites which are unaffected by late-stage fluids, carbonatites altered by late-stage fluids and carbo-hydrothermal veins (P&K = *Pokrovskii* and *Kravchenko*, 2001; *Zaitsev*, 1996; *Zaitsev* et al., 2002), see also text for explanation

Data of *Pokrovskii* and *Kravchenko* (2001) were obtained from different depths of boreholes at Khibina. Samples collected from depths >500 m show no alteration, whereas samples from depths <500 m show significant stable isotope changes (in $\delta^{13}C$, $\delta^{18}O$ as well as in $\delta^{34}S$ values). Pseudomorphs formed during alteration of primary burbankite (also shown in Fig. 4) have elevated $\delta^{13}C$ and $\delta^{18}O$ values that have been interpreted as a result of interaction with carbonatite-related fluid (*Zaitsev* et al., 2002).

C and O isotope data from the dykes are enclosed in a field of altered carbonatites and partly also in a field of hydrothermal veins, suggesting a similar origin to these late-stage carbonate formations. Monchiquite sample 625/218.8 plots far away from all available data for the Khibina rocks with significant ^{18}O enrichment. The high $\delta^{18}O$ value indicates low temperature carbonate formation or interaction with an ^{18}O-enriched fluid. However, the present data set is not appropriate to explore the responsible processes in further detail.

Sr–Nd isotope composition

Analytical procedures for Sr–Nd-isotope analyses are reported in *Zaitsev* et al. (2002) and in the electronic supplement. Initial $^{87}Sr/^{86}Sr$ and $^{143}Nd/^{144}Nd$ ratios were calculated for an age of 370 Ma (*Kramm* and *Kogarko*, 1994). The $(^{87}Sr/^{86}Sr)_{370}$ ratios in the monchiquites display a wide scatter – ranging between 0.70360 and 0.70393. The $(^{87}Sr/^{86}Sr)_{370}$ ratio of the nephelinite sample falls within this range (0.70364) while the phonolite value of 0.70401 is higher than the range defined by the monchiquites. The $(^{143}Nd/^{144}Nd)_{370}$ ratios are also variable between 0.51225 and 0.51237 for the monchiquites while the ratios for the nephelinite and phonolite are 0.51231 and 0.51228 respectively. One phonolite (KH 370) spatially associated with the carbonatites has a $(^{87}Sr/^{86}Sr)_{370}$ ratio of 0.70392 and a $(^{143}Nd/^{144}Nd)_{370}$ ratio of 0.51233 (*Kramm* and *Kogarko,* 1994).

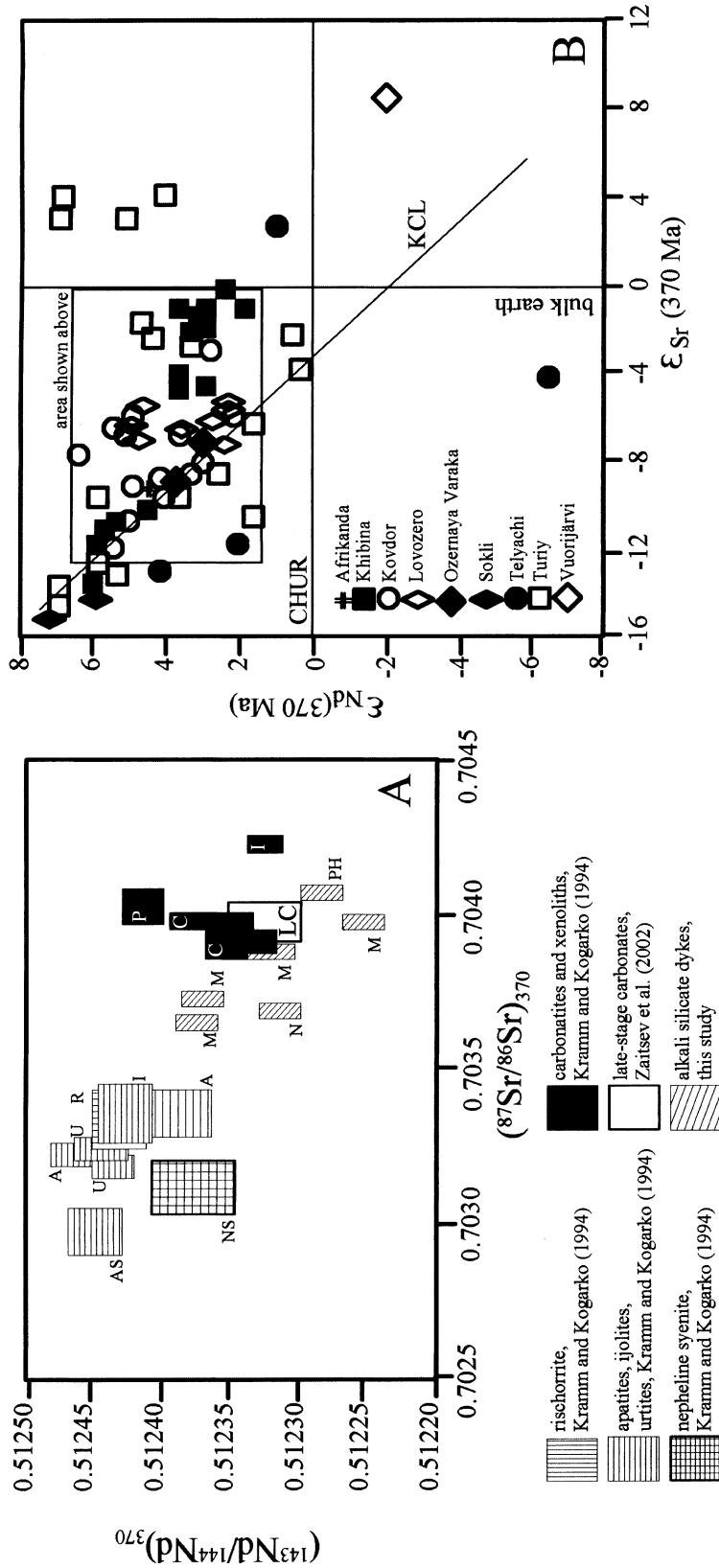Fig. 5. **A** Plot of $(^{143}Nd/^{144}Nd)_{370}$ *vs.* $(^{87}Sr/^{86}Sr)_{370}$ for the Khibina alkali silicate rocks and carbonatites (present study, *Kramm* and *Kogarko*, 1994; *Zaitsev* et al., 2002). Abbreviations: *A* apatite–nepheline rock, *AS* apatite–titanite rock (both are associated with ijolite–urtites), *C* carbonatite, *I* ijolite, *LC* late stage carbonatite, *M* monchiquite, *N* nephelinite, *NS* nepheline syenite, *P* pyroxenite, *PH* phonolite. **B** ε – plot showing isotope data of occurrences of the Kola Alkali Province compiled from *Kramm* (1993), *Kramm* and *Kogarko* (1994), *Dunworth* and *Bell* (2001), *Zaitsev* et al. (2002). *KCL* Kola Carbonatite Line sensu *Dunworth* and *Bell* (2001)

Both values fall within the observed range for Sr and Nd ratios from our samples. On the $^{87}Sr/^{86}Sr$–$^{143}Nd/^{144}Nd$ diagram (Fig. 5) monchiquite, nephelinite and phonolite define a relatively broad elliptical field with a negative correlation similar to that observed for other Kola alkaline–carbonatite complexes (e.g. *Kramm*, 1993; *Kramm* and *Kogarko*, 1994; *Dunworth* and *Bell*, 2001; *Zaitsev* et al., 2002). The $(^{87}Sr/^{86}Sr)_{370}$ ratios of the dyke rocks are markedly higher compared to the nepheline syenite foyaite and ijolite urtite, but they partly overlap with the range defined by the carbonatites and xenolitic pyroxenite and ijolite. The $(^{143}Nd/^{144}Nd)_{370}$ signatures of the dykes are similar to those from carbonatites and some plutonic rocks. The samples 630/186.3 and 695/124.5 show the lowest Nd-isotope ratios in the complex (Table 2).

The presence of late-stage REE-Sr-bearing carbonates in all of the monchiquite samples may indicate that the Sr–Nd-isotope signatures are the result of mixing between Sr- and Nd from magmatic sources and from carbothermal fluids. The $(^{87}Sr/^{86}Sr)_{370}$ and $(^{143}Nd/^{144}Nd)_{370}$ ratios of the Khibina carbonatites (including late-stage carbonates with abundant secondary REE-Sr-rich mineralization) are relatively homogeneous (*Zaitsev* et al., 2002) and it is assumed that the carbonates in the monchiquites have similar signatures. Samples 625/218.8 and 695/124.5 that have the largest amount of REE-Sr–Ba carbonates have $(^{87}Sr/^{86}Sr)_{370}$ signatures closest to those of the late stage carbonates (*Zaitsev* et al., 2002). Consequently, the $(^{87}Sr/^{86}Sr)_{370}$ ratios of samples 625/218.8 and 695/124.5 could be the result of late stage carbothermal fluid rock interaction (also suggested by the elevated $\delta^{18}O$ value of the carbonate of sample 625/218.8). However, both samples have the highest Rb/Sr-ratios of all monchiquites which is less consistent with the idea of being the result of a carbothermal alteration.

Sample 695/124.5 displays a marked difference in the $(^{143}Nd/^{144}Nd)_{370}$ ratio that is quite unlike the Nd-isotopic signature of the carbonates. Furthermore, with the exception of sample 625/118.9 there is no variation of the Sm/Nd ratio suggesting that there is no significant partitioning and mobilization of these elements involved in the formation of late-stage carbonates. It is assumed that the Sr- and Nd-isotope signatures of the dyke rocks mainly are the product of magmatic processes.

Discussion

Any discussion about the origin of the alkali silicate dykes must address their genetic relationship with the carbonatite dykes that occur in spatial proximity. The presence of euhedral and/or globular carbonates in the monchiquites could indicate a genetic relationship between the monchiquites and the carbonatite. The marked Sr- and Nd-isotopic difference between the carbonatites and most of the monchiquites (Fig. 5) argues strongly against a genetic relationship between the two. The globular carbonates show rims of mica and pyroxene ± magnetite. Commonly such features result from reaction between the silica-free carbonate and the alkali silicate rock (*Lucido* et al., 1980). The simplified reaction for the formation of diopside ($CaCO_3 + 2SiO_2 + MgO \Leftrightarrow CaMgSi_2O_6 + CO_2$) show that CO_2 can be released which may then be dissolved in the melt. The disequilibrium shown by the reaction rim leads to the conclusion that the globular carbonates were incorporated, probably as solid particles, into the monchiquites. In addition to the isotopic evidence this also

precludes a cogenetic magmatic evolution for the Khibina carbonatites and monchiquites, either by fractionation or liquid immiscibility. The feasibility of monchiquites incorporating calcite from carbonatites is shown by *Dudkin* et al. (1984), who described two monchiquite dykes crosscutting calcite carbonatites.

Besides the globular calcite and calcite phenocrysts, the silicate dykes contain disseminated groundmass carbonate that may derive from migration of late-stage fluids. The C and O isotope compositions of the bulk carbonate of the dyke rocks are within the field of hydrothermally altered carbonatite suggesting low temperature processes in carbonate formation. Low temperature interaction with low-δ^{18}O meteoric water may explain the high δ^{18}O values of bulk rock carbonate, but the close spatial association with carbonatites would favour the influence of carbonatitic fluids. Given that bulk rock carbonate was analysed, the stable isotope compositions may reflect different processes. Incorporation of carbonatitic material into the monchiquitic magma is assumed on the basis of textural and mineralogical observations. This process may either result in low or elevated δ^{13}C values depending on the nature (unaltered or altered by carbothermal fluid, respectively) of the assimilated carbonatite. Furthermore, the dykes may have served as conduits for migrating fluids, and the carbonatite-related fluids that caused alteration in the carbonatite may have also affected the monchiquite dykes.

As was pointed out above, the monchiquites and associated carbonatites should not be considered cogenetic. Rather, both are probably products of low-degree partial melting of a carbonated mantle peridotite (e.g. *Dalton* and *Presnall*, 1998; *Harmer*, 1999; *Lee* and *Wyllie*, 2000). In the following sections, the origin of the monchiquite (and nephelinite and phonolite) dykes is explored in more detail, without further considering the carbonatites.

The chemical and isotopic differences of the monchiquites can either be explained as resulting from an open-system behaviour (I) or reflecting source heterogeneity (II). Although neither of these models contradicts the other, they will be discussed as two separate scenarios here for the sake of simplicity.

Open-system process

The abrupt change in equilibrium of the magma at crustal levels as indicated by the chemical and textural features of pyroxenes, advocates against a steady AFC-process but points to distinct stages of disequilibrium due to intermittent stages of fractionation, assimilation or magma mixing. Such scenario is discussed in the following parts.

Most of the monchiquite samples define a good correlation between CaO and MgO. This could be explained by fractionation of 10 to 20 wt.-% of olivine from a picrite magma such as sample 604/400p (Fig. 3). The CaO–MgO-concentrations of samples 699/255.6 and 596/418.2 could also be caused by magnetite fractionation after olivine fractionation. However, whereas olivine fractionation roughly accounts for the variations of CaO, MgO and Al_2O_3, the variations seen in some of the other elements (e.g. TiO_2, Na_2O, Rb, Th, Y) is difficult to explain. This could be the result of intermittent episodes of magma mixing or selective wall-rock assimilation as furthermore evidenced by heterogeneities in radiogenic isotope signatures and pyroxene composition.

Within the spectrum of $(^{87}Sr/^{86}Sr)_{370}$- and $(^{143}Nd/^{144}Nd)_{370}$ – ratios from the Khibina complex the monchiquites are situated at lower Nd- and higher Sr-signatures compared to the majority of the nepheline syenitic rocks.

Such findings can be explained in two different ways (A and B), neither of which exclude prior steps of mineral fractionation: In the first (A), the monchiquites (or their primary picritic magma) originally had Sr- and Nd-isotopic signatures similar to those of the nepheline syenites which predominate in the complex (Fig. 5) but the melts then became contaminated by material with lower radiogenic Nd- and higher radiogenic Sr-isotopic signatures. This material could be either (1) Precambrian crustal wall rock and/or (2) carbonatite or other alkali silicate rocks such as the ijolite or pyroxenite which occur as xenoliths in carbonatite (I and P in Fig. 5, see also *Kramm* et al., 1993; *Kramm* and *Kogarko*, 1994).

According to a second explanation (B) the primary monchiquitic magma originally had Sr–Nd-signatures similar to those of the carbonatites. Mixing with nepheline syenitic melts or assimilation of plutonic rocks of the Khibina complex, the isotopic compositions of the monchiquites could have been shifted to lower radiogenic Sr and higher radiogenic Nd-signatures.

Explanation A involves either assimilation of crustal wall rock or the reaction/ assimilation of carbonatites. According to a calculation presented in Table 3 (A, B, C) assimilation of partly extremely high (>50%) amounts of Precambrian gneiss in a hypothetical primary picritic magma would be needed in order to produce the concentration and isotopic signatures of samples 699/255.6 and 695/124.5 which define the isotopic variation found in the monchiquites. The variable amounts of assimilated wall rock resulting from the calculation make such scenario appear unrealistic. For example assimilation of >70% of wall rock is needed in order to explain the $^{143}Nd/^{144}Nd$-signatures and of >30% to explain the MgO-concentrations. However, the SiO_2 contents of the contaminated melts don't agree with the primitive character of the monchiquites. Such finding clearly rules out crustal contamination as an effective process, unless one assumes intensive steps of fenitization prior to assimilation of Precambrian crustal rocks (*Kramm*, 1994; *Sindern* and *Kramm*, 2000). However, there is no indication from the xenoliths that extensively fenitized crustal rocks contributed to the magmatic products at Khibina.

This leaves, for explanation A, the possibility of interaction of the monchiquites with carbonatites or ijolites as the main mechanism. There is petrographic evidence showing the reaction of calcite, presumably coming from the carbonatites, with the monchiquite melt to mafic minerals. Sr and Nd from the carbonatite could also be incorporated into the monchiquitic melt. A picritic or monchiquitic melt with primary Sr- and Nd-elemental and isotopic characteristics according to scenario I (i.e. similar to isotope characteristics of the nepheline syenites, ijolites, urtites, apatitites) could be changed so that it would end up with the isotopic and concentration signatures of samples 699/255.6 and 596/418.2. This could be produced by assimilation of varying amounts of ijolite or carbonatite (3.6 to 72.4% of ijolite or 67.3 to 87.5% of carbonatite, see Table 3, D, E). Here, too, the large variability of assimilated amounts necessary to explain the different element and isotope compositions make simple assimilation of carbonatites or ijolite unlikely.

Figure 5 and Table 2 make clear that any such assimilation process could only account for the isotopic signatures of samples 699/255.6 and 596/418.2 which are

Table 3. *Mixing calculations according to open system scenario I. Assimilation of rocks A to E in a hypothetic picritic primary magma. Characteristics of primary picritic magma: $Sr = 2741\,ppm$, $({}^{87}Sr/{}^{86}Sr)_{370} = 0.70299$, $Nd = 342\,ppm$, $({}^{143}Nd/{}^{144}Nd)_{370} = 0.51244$, $SiO_2 = 35\,wt.\text{-}\%$, $MgO = 16.75\,wt.\text{-}\%$, values chosen according to data of Kramm and Kogarko (1994). * Calculation based on isotopic ratios only, fractions are expressed as Mol-fractions. Further explanation in the text*

		Hypothetic mixture 1, Comparable to monchiquite 699/255.6	Amount (wt.-%) of assimilated rock necessary to produce element or isotopic signatures of mixture 1	Hypothetic mixture 2, Comparable to monchiquite 695/124.5	Amount (wt.-%) of assimilated rock necessary to produce element or isotopic signatures of mixture 2
Assimilated rock A	Gneiss SI 6				
Sr (ppm)	388	2581	6.7%	2367	15.8%
$({}^{87}Sr/{}^{86}Sr)_{370}$	0.72304	0.70367		0.70400	
Nd (ppm)	35.2	113.1		117.4	
$({}^{143}Nd/{}^{144}Nd)_{370}$	0.51022	0.51237	74.6%	0.51225	73.2%
SiO_2 (wt.-%)	73.22	37.09	5.5	38.90	10.2
MgO (wt.-%)	0.43	7.52	56.6	11.33	33.2
Assimilated rock B	Gneiss SI 77				
Sr (ppm)	129	2581	6.1	2367	14.3%
$({}^{87}Sr/{}^{86}Sr)_{370}$	0.78177	0.70367		0.70400	
Nd (ppm)	47.0	113.1		117.4	
$({}^{143}Nd/{}^{144}Nd)_{370}$	0.51056	0.51237	77.6	0.51225	76.1%
SiO_2 (wt.-%)	74.75	37.09	5.3	38.90	9.8
MgO (wt.-%)	0.22	7.52	47.3	11.33	32.8
Assimilated rock C	Qz-Fenite SI 7.2				
Sr (ppm)	210	2581	6.2	2367	14.7%
$({}^{87}Sr/{}^{86}Sr)_{370}$	0.72829	0.70367		0.70400	
Nd (ppm)	2.9	113.1		117.4	
$({}^{143}Nd/{}^{144}Nd)_{370}$	0.51037	0.51237	67.5	0.51225	66.2%
SiO_2 (wt.-%)	70.03	37.09	6.0	38.90	11.1
MgO (wt.-%)	0.63	7.52	57.3	11.33	33.6

Table 3 (continued)

Table 3 (continued)

	Hypothetic mixture 1, Comparable to monchiquite 699/255.6	Amount (wt.-%) of assimilated rock necessary to produce element or isotopic signatures of mixture 1	Hypothetic mixture 3, Comparable to monchiquite 596/418.2	Amount (wt.-%) of assimilated rock necessary to produce isotopic signatures of mixture 2
Assimilated rock D	Ijolite, KH 1029			
Sr (ppm)	1594		2697	
$(^{87}Sr/^{86}Sr)_{370}$	0.70425	2581 0.70367 13.8	0.70375	3.6
Nd (ppm)	104.3	113.1	276.5	
$(^{143}Nd/^{144}Nd)_{370}$	0.51232	0.51237 58.3*	0.51237	58.3*
SiO$_2$ (wt.-%)	42.00	37.09 29.9	34.79	–
MgO (wt.-%)	4.00	7.52 72.4	12.40	34.1
Assimilated rock E	Carbonatite, KH 6			
Sr (ppm)	26249	2581	2697	
$(^{87}Sr/^{86}Sr)_{370}$	0.70400	0.70367 67.3*	0.70375	75.2*
Nd (ppm)	621	113.1	276.5	
$(^{143}Nd/^{144}Nd)_{370}$	0.51236	0.51237 87.5*	0.51237	87.5*

Table 4. *Fractionation- and mixing calculations illustrating scenario I B. Distribution coefficients for calculation of Sr and Nd fractionation from* Morbidelli *et al. (2000)*

	a	b	b + c		c
A	Primary magma, with picritic composition and isotopic characteristics similar to monchiquite 695/124.5	Calculated after fractionation of 10.4 wt-% of olivine from primary magma	48% c 52% b	For comparison to actual samples: 625/218.8	Nepheline Syenite similar to KH 9445, 9502, 8121, 8129, 8119 (Kramm & Kogarko 1994)
SiO_2	35.01	34.58	44.37	41.51	54.98
MgO	16.75	12.96	7.09	12.83	0.73
Sr	2741	3055	2596.6	1462	2100
Nd	342	381	270	93.7	150
$^{87}Sr/^{86}Sr$	0.70393	0.70393	0.70357	0.70390	0.70299
$^{143}Nd/^{144}Nd$	0.51225	0.51225	0.51230	0.51232	0.51244
B	Primary magma, with picritic composition and isotopic characteristics similar to monchiquite 695/124.5	Calculated after fractionation of 20.7 wt.-% of olivine from primary magma	28% c 72% b	596/418.2	Nepheline Syenite similar to KH 9445, 9502, 8121, 8129, 8119 (Kramm & Kogarko 1994)
SiO_2	35.01	33.74	39.68	34.79	54.98
MgO	16.75	8.07	6.01	12.40	0.73
Sr	2741	3448	3071	2697	2100
Nd	342	430	352	276.5	150
$^{87}Sr/^{86}Sr$	0.70393	0.70393	0.70375	0.70375	0.70299
$^{143}Nd/^{144}Nd$	0.51225	0.51225	0.51227	0.51237	0.51244

characterized by highest $(^{143}Nd/^{144}Nd)_{370}$ – signatures. All other samples have $(^{143}Nd/^{144}Nd)_{370}$ – ratios as low or lower than the lowest ratios known from rocks of the massif. Consequently, contamination of monchiquite or phonolite magma by carbonatites can't be an important process in the evolution of the dyke rocks.

Explanation B for an open system process is the assimilation of the dominant rocks within the complex (nepheline syenite, ijolite, urtite) or admixture of such magmas to picritic magma originally having isotopic signatures close to that of the carbonatites. For evaluation of this model, we take an average of the isotopic signatures of the nepheline syenites and ijolites (given by samples KH 8119, 8121, 8129 of *Kramm* and *Kogarko*, 1994, see also Fig. 5). Ne–Syenite KH 9445 (*Kramm* and *Kogarko*, 1994), is taken as representative of the chemical

composition of the "contaminant". The model assumes fractionation of olivine according to Fig. 3 and subsequent admixture of a ne–syenitic magma. The mixing proportions are given according to the isotopic signatures of the monchiquites presumably produced by the mixing (Table 4).

The mixing calculation indicates a tendency to higher SiO_2 contents and clearly lower MgO contents than actually observed in the monchiquites. Due to the lower Nd/Sr-ratio in the nepheline syenites of the Khibina complex compared to the assumed primary picrite admixture of nepheline syenitic magmas may either explain the isotopic shift of a primary magma to lower radiogenic $^{87}Sr/^{86}Sr$- or to higher radiogenic $^{143}Nd/^{144}Nd$-ratios. However, comparing the results to the monchiquite samples it can be seen that admixture of a nepheline syenitic magma can't explain the visible covariation of both isotopic signatures in the monchiquites.

Consequently, although olivine-fractionation and mixing of different but chemically similar magmas must have occurred, as is indicated by the major element variation and the clinopyroxene structures, it can hardly explain the isotopic heterogeneity. Accordingly, this must be a primary feature which leads to scenario II (i.e. isotopic source heterogeneity).

Source heterogeneity

The isotopic heterogeneity can only be explained by primary heterogeneity. The source of the monchiquites as well as other dyke rocks which occur in a relatively small area in the eastern part of the complex must comprise small, isotopically distinct volumes. Thus, the formation of the monchiquite melts must have occurred simultaneously, within small mantle volumes characterized by different isotopic signatures.

On the basis of the observation that the Sr–Nd isotopic signatures of the alkaline silicate rocks, carbonatites and phoscorites from the Kola Alkaline Province are mainly aligned along a linear array (Fig. 5, Kola Carbonatite Line, KCL, *Kramm* (1993), *Dunworth* and *Bell* (2001)), but also show deviations from that array, at least four mantle components have to be distinguished.

The first component defining the upper end of the KCL was ascribed to a depleted mantle source by *Kramm* (1994). This would be consistent with the description of *Andersen* and *Sundvoll* (1995) who see evidence for a depleted Archean mantle beneath the Baltic shield. However, according to recent studies (*Beard* et al., 1998; *Dunworth* and *Bell*, 2001), the component defining the upper end of the KCL may best be explained as derived from a mantle plume. Mantle plume activity on Kola is indicated by the formation of more than 20 alkaline magmatic intrusions within a period of c. 20 Ma (*Kramm* et al., 1993; *Mahotkin* et al., 2000). It also explains the high $^3He/^4He$ ratios indicative of a lower mantle source found in the complexes of Kovdor, Sebl'yavr and Lesnaya Varaka (*Marty* et al., 1998). In addition, it has been shown for kimberlites and melilitites from Kola (*Beard* et al., 1998) but also for the large nepheline syenite intrusions from Khibina and Lovozero (Kola) that metasomatic scavenging of incompatible trace elements took place recently prior to melt formation (*Kramm* and *Kogarko*, 1994). This, too, strongly argues for the existence of a mantle plume.

The component defining the lower end of the KCL is characterized by slightly higher radiogenic Sr- and lower radiogenic Nd-isotopic ratios compared to bulk earth, and similar to EM I. From the Sr–Nd-isotopic point of view this component is not equivalent to a Devonian EM I-type component as described by *Dostal* et al. (1998) for an oceanic setting (*Dunworth* and *Bell*, 2001). Only a slight increase in Rb/Sr and decrease in Sm/Nd in a mantle domain beneath Kola would lead to a component defining the lower end of the KCL. This would also serve as the component of "shallower lithospheric origin" postulated by *Beard* et al. (1998) for the origin of Devonian kimberlites and melilitites from Kola.

The third component must be dominated by high $^{87}Sr/^{86}Sr$-ratios, similar to EM II (*Hofmann*, 1997), and the other one (fourth component) must be characterised by low $^{143}Nd/^{144}Nd$- and $^{87}Sr/^{86}Sr$- ratios (*Mahotkin* et al., 2000).

The alkali silicate dyke rocks discussed in this study show, like the other spatially associated magmatic products (carbonatites, xenolithic pyroxenite and ijolite), deviation from the KCL (*Kramm* and *Kogarko*, 1994; *Dunworth* and *Bell*, 2001). This indicates that the component enriched in radiogenic Sr must contribute significantly to the monchiquites and phonolites/nephelinites. *Zaitsev* et al. (2002) point out that the Khibina carbonates (whether primary carbonatitic or late stage) have typical mantle $\delta^{13}C$ values despite their elevated $^{87}Sr/^{86}Sr$ ratios. This implies that the component characterized by higher $^{87}Sr/^{86}Sr$ ratios contains no crustal carbon in significant amounts relative to other components. This might rule out a sedimentary origin for this mantle component, due to subduction of crustal material, unless a volatilization process can separate carbon from the subducted material (*Kerrick* and *Connolly*, 2001). Another process leading to an enriched mantle domain could be an older mantle metasomatic event.

A characteristic feature of the carbonatites, unlike the alkali silicate rocks of Khibina, is their somewhat limited Sr–Nd-isotopic variation (Fig. 5). This strongly favors a carbonatite derived from primary carbonatitic melts accumulated – and thus homogenized – from a larger volume. The field of Nd and Sr isotope data of carbonatites from Khibina displays the greatest offset from the KCL of all Khibina data. It is therefore postulated that the carbonatitic melt passes mantle volumes containing higher radiogenic Sr similar to EM II. Such mantle volumes could be composed of subducted crustal material. If this is the case, the carbon in the carbonatitic melt either predominates over sedimentary carbon or the latter is not mobilized in the carbonatitic melt or has been volatilized during subduction. This would explain the pristine $\delta^{13}C$-values but slightly enriched $^{87}Sr/^{86}Sr$-ratios of the carbonatites. Such reasoning can't be applied to all of the carbonatite occurrences of the KAP since the Nd and Sr isotopic signatures in other complexes vary over the range of isotopic signatures of the KAP (Fig. 5, *Kramm*, 1993; *Zaitsev* and *Bell*, 1995; *Dunworth* and *Bell*, 2001; *Zaitsev* et al., 2002).

Mantle metasomatism beneath the Khibina complex is indicated by metasomatized harzburgites found as xenoliths in Khibina (*Arzamastsev* and *Belyatskii*, 1999). As Rb–Sr-dating yields an age of 427 Ma for the metasomatic event, *Arzamastsev* and *Belyatskii* (1999) consider the Caledonian collision and subduction as the process which led to incorporation of crustal material beneath the Kola region.

Carbonatitic metasomatism by fluids in the sub-lithospheric mantle might also contribute to the isotopic heterogeneity seen in the data of the alkali silicate dyke

rocks from Khibina. The carbonatitic mantle metasomatism would thus be the process which incorporates the radiogenic (EMII-like) component into the Khibina rocks. Such process, however, doesn't account for all small-scale isotopic heterogeneities as the latter component doesn't represent one of the end-members of the KCL.

The process, most effective in producing small scale isotopic heterogeneity within the mantle seems to be plume activity. *Bell* (2001, 2002) has recently proposed an integrated model that relates carbonatites, lamprophyres and kimberlites to melting within an isotopically heterogeneous plume head, and *Bell* and *Tilton* (2002) have argued that most carbonatites are generated by plume activity. Several well known, presently active plumes, for example Iceland and Hawaii, are known to be isotopically heterogeneous (*Bell*, 2001), perhaps even zoned. The chemical differences observed among small volume melts is attributed by *Bell* (2002) to low-degree partial melting in the cooler parts of an isotopically heterogeneous, plume head. Depending on the degree of partial melting, the CO_2/H_2O ratio, and the abundance of volatiles, a wide range of small volume, volatile rich melts can be generated, each quite distinct yet related both spatially and temporally. Because of thermal entrainment of lower mantle during upward migration, a plume head can be both compositionally and thermally layered leading to small mantle volumes (*Campbell*, 1995) and discrete mantle domains. Given the complexities within plume heads (e.g. *Wyllie*, 1988), even fluids transporting components from the deeper mantle may interact with other mantle domains. Mixing between various melts generated within a plume head or melting involving one or more domains, coupled with fluid activity, can probably explain the small scale heterogeneity observed in rocks of the Kola alkaline province (*Bell*, 2002).

A possible scenario for an upwelling plume at Kola could involve enrichment of a depleted mantle (*Andersen* and *Sundvoll*, 1995) in LIL and HFS elements (*Dunworth* and *Bell*, 2001; *Bell*, 2002). Fluids within the plume head could interact with various mantle domains enhancing small scale isotopic heterogeneities.

Conclusions

The eastern part of the Khibina alkali complex is characterised by the occurrence of alkali silicate dykes (picrite, monchiquite, nephelinite, phonolite) spatially associated with carbonatite dykes. The presence of calcite in the monchiquite dykes could point to a cogenetic origin of monchiquite and carbonatite. However, textural evidence suggests that these are carbonates mechanically incorporated into the dykes from earlier carbonatites. The isotopic contrast between the monchiquites studied here and carbonatites (*Kramm* and *Kogarko*, 1994; *Zaitsev* et al., 2002) argues against a cogenetic magmatic relationship of both rocks either by fractionation or liquid immiscibility.

We have shown that minor olivine and magnetite fractionation leading to an evolution from picrite to monchiquite coupled with magma mixing probably occurred. The composition of clinopyroxenes indicates that part of these steps occurred in crustal levels. However, neither these processes nor mixing between picrite/monchiquite and Precambrian wall rocks or other magmatic products of the Khibina complex can explain all chemical and isotopic characteristics of the

monchiquites. Thus, these features we consider primary, indicative of the source region producing the picrites/monchiquites by low degree partial melting. Taking the small volume and limited area of occurrence of these dykes into consideration, the mantle domain forming the dyke magmas must be small.

Thus the four mantle components (1 depleted mantle, 2 plume component, 3 EMI-like component, 4 EMII-like component) were all involved but indifferent proportions and on a fairly small scale. The EMII-like component might be incorporated into the source areas of the primary magmas by carbonatitic fluids which passed through mantle domains containing subducted crustal material. The most probable process explaining small scale isotopic heterogeneity is plume activity.

Acknowledgements

References

Andersen T, Sundvoll B (1995) Neodymium isotope systematics of the mantle beneath the Baltic shield: evidence for depleted mantle evolution since the Archean. Lithos 35: 235–243

Aoki K, Shiba I (1973) Pyroxenes from lherzolite inclusions of Itinomegata, Japan. Lithos 6: 45–51

Arzamastsev AA, Belyatskii BV (1999) Evolution of the mantle source of the Khibiny Massif: evidence from Rb–Sr and Sm–Nd data on deep-seated xenoliths. Transact (Dokl) Russ Acad Sci/Earth Sci Sect 366, 3: 387–391 (in Russian)

Arzamastsev AA, Kaverina VA, Polezhaeva LI (1988) Dykes of the Khibina Massif and its Surroundings. Kola Science Centre Press, Apatity, 85 pp (in Russian)

Beard AD, Downes H, Vetrin VR, Kempton PD, Maluski H (1996) Petrogenesis of Devonian lamprophyre and carbonatite minor intrusions, Kandalaksha Gulf (Kola Peninsula, Russia). Lithos 39: 93–119

Beard AD, Downes H, Hegner E, Sablukov SM, Vetrin VR, Balogh K (1998) Mineralogy and geochemistry of Devonian ultramafic minor intrusions of the southern Kola Peninsula, Russia: implication for the petrogenesis of kimberlites and melilitites. Contrib Mineral Petrol 130: 288–303

Bell K (1998) Radiogenic isotope constrains on relationships between carbonatites and associated silicate rocks – a brief review. J Petrol 39: 1987–1996

Bell K (2001) Carbonatites: relationships to mantle-plume activity. In: *Ernst RE, Buchan KL* (eds) Mantle plumes: their identification through time. GSA Special Publication, pp 267–290

Bell K (2002) Carbonatites and related alkaline rocks, lamprophyres, and kimberlites – indicators of mantle-plume activity. Role of superplumes in the Earth System. International Workshop, Tokyo, January 2002. Abstract 16: 365–368

Bell K, Blenkinsop J (1987) Archean depleted mantle: evidence from Nd and Sr initial isotopic ratios of carbonatites. Geochim Cosmochim Acta 51: 291–298

Bell K, Tilton GR (2002) Probing the mantle: the story from carbonatites. Eos v 83

Bultitude RJ, Green DH (1971) Experimental study of crystal-liquid relationships at high pressure in olivine nephelinite and basanite compositions. J Petrol 12: 121–147

Campbell IH (1998) The mantle's chemical structure: insights from the melting products of mantle plumes. In: *Jackson I* (ed) The Earth's mantle. Cambridge University Press, Cambridge, pp 259–310

Dahlgren S (1994) Late Proterozoic and Carboniferous ultramafic magmatism of carbonatitic affinity in southern Norway. Lithos 31: 141–154

Dalton JA, Presnall DC (1998) The continuum of primary carbonatitic-kimberlitic melt compositions in equilibrium with lherzolite: data from the system $CaO–MgO–Al_2O_3–SiO_2–CO_2$ at 6 Gpa. J Petrol 39: 1953–1964

Dobosi G, Fodor RV (1992) Magma fractionation, replenishment, and mixing as inferred from green-core clinopyroxenes in Oligocene basanite, southern Slovakia. Lithos 28: 133–150.

Dostal J, Cousens B, Dupuy C (1998) The incompatible element characteristics of an ancient subducted sedimentary component in Ocean Island Basalts from French Polynesia. J Petrol 39: 937–952

Duba A, Schmincke HU (1985) Polybaric differentiation of alkali basaltic magmas: evidence from green-core clinopyroxenes (Eifel, FRG). Contrib Mineral Petrol 91: 340–353

Dudkin OB, Minakov FV, Kravchenko MP, Kravchenko EV, Kulakov AN, Polezhaeva LI, Pripachkin VA, Pushkarev YuD, Rungenen GI (1984) Khibina carbonatites. Academy of Sciences of the USSR, Apatity (in Russian)

Dunworth EA, Bell K (2001) The Turiy massif, Kola peninsula, Russia: isotopic and geochemical evidence for multi-source evolution. J Petrol 42: 377–405

Grove TL, Barker MB (1984) Phase equilibrium controls on the tholeitic versus calc-alkaline differentiation trends. J Geophys Res 89: 3253–3279

Harmer RE (1999) The petrogenetic association of carbonatite and alkaline magmatism: constraints from the Spitskop Complex, South Africa. J Petrol 40: 525–548

Harmer RE, Gittins J (1998) The case for primary, mantle-derived carbonatite magma. J Petrol 39: 1895–1903

Harmer RE, Lee CA, Eglington BM (1998) A deep mantle source for carbonatite magmatism: evidence from the nephelinites and carbonatites of the Buhera district, SE Zimbabwe. Earth Planet Sci Lett 158: 131–142

Hofmann AW (1997) Mantle geochemistry: the message from oceanic volcanism. Nature 385: 219–229

Ivanikov VV, Rukhlov AS, Bell K (1998) Magmatic evolution of the melilite-carbonatite-nephelinite dyke series of the Turiy peninsula (Kandalaksha Bay, White See, Russia). J Petrol 39: 2043–2059

Kerrick DM, Connolly JAD (2001) Metamorphic devolatilization of subducted oceanic metabasalts: implications for seismicity, arc magmatism and volatile recycling. Earth Planet Sci Lett 189: 19–29

Khomyakov AP (1995) Mineralogy of hyperagpaitic alkaline rocks. Clarendon Press, Oxford, 220 pp

Kogarko LN (1997) Role of CO_2 on differentiation of ultramafic alkaline series: liquid immiscibility in carbonatite-bearing phonolitic dykes (Polar Siberia). Mineral Mag 61: 549–556

Kostyleva-Labuntsova EE, Borutsky BE, Sokolova MN, Shlukova ZV, Dorfman MD, Dudkin OB, Kozyreva LV, Ikorsky SV (1978) Mineralogy of the Khibina Massif. Nauka, Moscow, 228 pp

Kramm U (1993) Mantle components of carbonatites from the Kola Alkaline Province, Russia and Finland: a Nd–Sr study. Eur J Mineral 5: 985–989

Kramm U (1994) Isotope evidence for ijolite formation by fenitization: Sr–Nd data of ijolites of the type locality Iivaara, Finland. Contrib Mineral Petrol 115: 279–286

Kramm U, Kogarko LN (1994) Nd and Sr isotope signatures of the Khibina and Lovozero agpaitic centres, Kola Alkaline Province, Russia. Lithos 32: 225–242

Kramm U, Kogarko LN, Kononova VA, Vartiainen H (1993) The Kola Alkaline Province of the CIS and Finland: precise Rb–Sr ages define 380–360 Ma age range for all magmatism. Lithos 30: 33–44

Lee WJ, Wyllie PJ (2000) The system CaO–MgO–SiO$_2$–CO$_2$ at 1 Gpa, metasomatic wehrlites, and primary carbonatitic magmas. Contrib Mineral Petrol 138: 214–228

Lucido G, Nuccio PM, Leone G, Longinelli A (1980) Amygdaloidal basalts: isotopic and petrographic evidence for non-diagenetic crustal source of carbonate inclusions. Tschermaks Mineral Petrol Mitt 27: 113–128

Mahotkin IL, Gibson SA, Thompson RN, Zhuravlev DZ, Zherdev PU (2000) Late Devonian diamondiferous kimberlite and alkaline picrite (proto-kimberlite?) magmatism in the Arkhangelsk region, NW Russia. J Petrol 41: 201–227

Marty B, Tolstikhin I, Kamensky IL, Nivin V, Balaganskaya E, Zimmermann JL (1998) Plume-derived rare gases in 380 Ma carbonatites from the Kola region (Russia) and the argon isotopic composition in the deep mantle. Earth Planet Sci Lett 164: 179–192

Morbidelli L, Gomes CB, Brotzu P, D'Acquarica S, Garbarino C, Ruberti E, Traversa G (2000) The Pariquera Acu K-alkaline complex and southern Brazil lithospheric mantle source characteristics. J Asian Earth Sci 18: 129–150

Pearce NJG, Leng MJ (1996) The origin of carbonatites and related rocks from the Igaliko Dyke Swarm, Gardar Province, South Greenland: field, geochemical and C–O–Sr–Nd isotope evidence. Lithos 39: 21–40

Pokrovskii BG, Kravchenko SM (2001) Stable isotopes in the Khibiny and Lovozero Massifs: magma sources and conditions of the postmagmatic alterations. Geochem Int 39: 88–98

Rock NMS (1991) Lamprophyres. Blackie, Glasgow, 285 pp

Simonetti A, Bell K (1994) Isotopic and geochemical investigation of the Chilwa Island carbonatite complex, Malawi: evidence for a depleted mantle source region, liquid immiscibility and open-system behaviour. J Petrol 35: 1597–1621

Simonetti A, Shore M, Bell K (1996) Diopside phenocrysts from nephelinite lavas, Napak volcano, eastern Uganda: evidence for magma mixing. Can Mineral 34: 411–421

Sindern S, Kramm U (2000) Volume characteristics and element transfer of fenite aureoles: a case study from the Iivaara alkaline complex, Finland. Lithos 51: 75–93

Sokolov SV (1985) Carbonates in ultramafite, alkali-rock, and carbonatite intrusions. Geochem Int 22: 150–166

Wakita H, Rey P, Schmitt RA (1971) Abundances of the 14 rare-earth elements and 12 other trace-elements in Apollo 12 samples: five igneous and one breccia rocks and four soils. Proceedings, Second Lunar Science Conference. Geochim Cosmochim Acta [Suppl] 2: 1319–1329

Wass SY (1979) Multiple origin of clinopyroxenes in alkali basaltic rocks. Lithos 12: 115–132

Wood DA, Joron JL, Treuil M, Norry M, Tarney J (1979) Elemental and Sr isotope variations in basic lavas from Iceland and surrounding ocean floor. Contrib Mineral Petrol 70: 319–339

Wyllie P (1988) Solidus curves, mantle plumes, and magma generation beneath Hawaii. J Geophys Res 93: 4171–4181

Zaitsev AN (1996) Rhombohedral carbonates from carbonatites of the Khibina massif, Kola peninsula, Russia. Can Mineral 34: 453–468

Zaitsev A, Bell K (1995) Sr and Nd isotope data of apatite, calcite and dolomite as indicators of the source and the relationships of phoscorites and carbonatites from the Kovdor massif, Kola peninsula, Russia. Contrib Mineral Petrol 121: 324–335

Zaitsev AN, Chakhmouradian AR (2002) Calcite-amphibole-clinopyroxene rock from the Afrikanda complex, Kola Peninsula, Russia: mineralogy and possible link to carbonatites. II. Oxysalt minerals. Can Mineral 40: 103–200

Zaitsev AN, Wall F, LeBas MJ (1998) REE-Sr–Ba minerals from the Khibina carbonatites, Kola peninsula, Russia: their mineralogy, paragenesis and evolution. Mineral Mag 62: 225–250

Zaitsev AN, Demény A, Sindern S, Wall F (2002) Burbankite group minerals and their alteration in rare earth carbonatites-source of elements and fluids (evidence from C–O and Sr–Nd isotopic data). Lithos 62: 15–33

Authors' addresses: *S. Sindern* and *U. Kramm*, Institut für Mineralogie und Lagerstättenlehre – RWTH-Aachen, Wüllnerstrasse 2, D-52056 Aachen, Germany, e-mail: sindern@rwth-aachen.de; kramm@rwth-aachen.de; *A. N. Zaitsev*, Department of Mineralogy, St. Petersburg State University, 7/9 University Emb., St. Petersburg, 199034, Russia, e-mail: anatoly@ AZ1562.spb.edu; *A. Demény*, Laboratory for Geochemical Research, Hungarian Academy of Sciences, Budaörsi út. 45, 1112 Budapest, Hungary, e-mail: demeny@geochem.hu; *K. Bell* and *A. S. Rukhlov*, Ottawa-Carleton Centre for Geoscience Studies, Department of Geology, Carleton University, Ottawa, Ontario, K1S 5B6, Canada, e-mail: arukhlov@ ccs.carleton.ca; *A. R. Chakmouradian*, Department of Geological Sciences, University of Manitoba, 125 Dysart Road, Winnipeg, Manitoba R3T 2N2, Canada; *J. Moutte*, Ecole des Mines, Centre SPiN, 158 Cours Fauriel, F-42100 Saint Etienne, France